

# Structural Performance of RC Beams Strengthened with NSM-CFRP

Abdelkrim Laraba<sup>1</sup>, Abdelghani Merdas<sup>2</sup>, Nasr-Eddine Chikh<sup>3</sup>

**Abstract**—An experimental work was performed to characterize the laminate and rods to concrete bond behavior based on pullout-bending tests. The structural performance of RC beams was assessed through loading to failure in a 4 points flexural test. The influences of the concrete strength, the type and the configuration of the reinforcement, and the embedded length on the bond behavior between the three materials (concrete, epoxy adhesive and CFRP) were evidenced and compared.

**Index Terms**— RC Beam, bond, bending, NSM-CFRP

## I. INTRODUCTION

An increasing number of RC structures have reached the end of their service life, either due to deterioration of the concrete and reinforcements caused by environmental factors, or due to an increase in applied loads. These deteriorated structures may be structurally deficient or functionally obsolete and most are now in serious need of extensive rehabilitation. CFRP sheets or plates are well suited to this application because of their high strength-to-weight ratio, good fatigue properties and excellent resistance to corrosion. Their application in civil engineering structures has been growing rapidly in recent years, because CFRPs are quickly and easily applied, their use minimizes labor costs and can lead to significant savings in the overall costs of a project. The Near Surface Mounted (NSM) technique has been used in recent years for the strengthening of reinforced concrete beams [1]-[3]. It involves the insertion of strips or rods of carbon fibers reinforced polymers (CFRP) in grooves made previously in the concrete cover of corresponding surfaces, filled with epoxy adhesive for fixation. Several experimental tests indicated benefits of NSM technique such performance of the NSM technique seems to be controlled entirely by the bond behavior of the interface laminate-adhesive-concrete, [4]-[7]. Test results on beam specimens indicated that application of the NSM FRP strips/rods significantly increased the load bearing capacity and improved the stiffness of the beams [8]-[10]. Although some interesting experimental studies have been developed, the structural behaviour of damaged RC elements

strengthened with NSM FRP rods still needs to be fully investigated. For this purpose, an experimental investigation has been carried out through pullout-bending tests. The influence of the following parameters has been considered: type of concrete, bond length, type of reinforcement and configurations type strengthening. Four-point bending tests were also performed on RC beams considering experimental variables such as: the type of reinforcement, the ratio of CFRP reinforcement. The recorded response of the specimens is presented and discussed and the measured strength and deflection of the specimens are estimated to assess the overall structural behavior of the strengthened concrete beam.

## II. STUDY OF THE BOND BEHAVIOUR

The influence of the following parameters has been considered:

- Type of concrete: two ordinary concretes (C30, C50) and one high performance concrete (HPC75).
- Bond length  $L_b$ : 120mm, 80mm and 40 mm.
- Type of reinforcement: smooth carbon rod (SCR) and smooth carbon plate (SCP).

Two configurations (Fig.1) were considered for the last reinforcing technique:

- A plate fully inserted in the groove (SCPF).
- A plate partially inserted in the groove (SCPP). This situation simulates the case of insufficient concrete cover depth or the case where the cutting of the bottom transverse steel is to be avoided. Obviously, a new layer of repairing concrete will be bonded to the existing concrete.

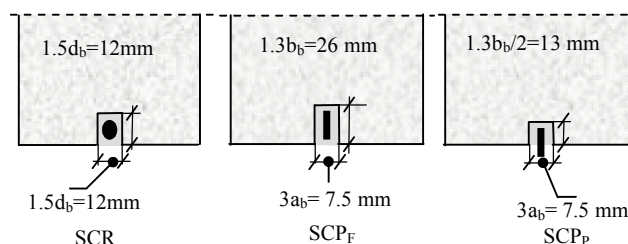


Fig.1 CFRP reinforcement configurations

### A. Materials Properties

#### 1. Carbon reinforcements (plate and rod)

CFRP plates and rods are composed of unidirectional carbon fiber embedded in epoxy adhesive matrix. They have similar cross section of  $50\text{mm}^2$ . To evaluate the tensile strength and the Young's modulus, uniaxial tensile tests were conducted with 200 kN maximum capacity hydraulic tensile machine. The following values of 2500 MPa, 160 GPa and 1.50%, represent respectively, the tensile strength, the

Abdelkrim Laraba<sup>1</sup> is with the Civil Engineering Department, Laboratory of Materials and Durability of Constructions (L.M.D.C), University of Constantine 1, Constantine 25000, Algeria, (e-mail: laraba\_ab@yahoo.fr).

Abdelghani Merdas<sup>2</sup> is Civil Engineering Department, Laboratory of Materials and Durability of Constructions (L.M.D.C), University of Sétif, Sétif 19000, Algeria, (e-mail: abdelghani.merdas@yahoo.com).

Nasr-Eddine Chikh<sup>3</sup> is with the Civil Engineering Department, Laboratory of Materials and Durability of Constructions (L.M.D.C), University of Constantine 1, Constantine 25000, Algeria, (e-mail: chikh\_ne@yahoo.fr).

Young's modulus and the ultimate strain at break of the composite.

2. Epoxy resin

EPONAL 371 was the type of resin used for filling grooves. Its properties according to the manufacturer are given in Table I.

TABLE I  
EPONAL 371 PROPERTIES

Type of epoxy adhesive	EPONAL 371
Tensile strength (MPa)	31.7 ±3.2
Elongation at break (%)	1.2 ± 0.3
Young's modulus (MPa)	3800 ±130

3. Concretes

Three types of vibrated concretes were studied: two ordinary concretes (C30) and (C50) and one high performance concrete (HPC75). All the results are gathered in Table II.

TABLE II  
MECHANICAL PROPERTIES OF CONCRETES

Constituents	C30	C50	HPC75
Compressive strength $f_{cm}$ (MPa)	37.5	57	73.5
Tensile strength $f_{ctm}$ (MPa)	2.97	4.73	6.01
Modulus of elasticity $E_c$ (GPa)	33.55	40,56	47.88

B. EXPERIMENTAL METHODOLOGY

The specimens were prepared at the age of 28 days. The two blocks composing each specimen were removed from the curing room to make the grooves using a table-mounted circular saw. Before bonding the CFRP, the grooves were again cleaned by compressed air (Fig. 2). To avoid epoxy adhesive in undesirable zones, a masking procedure was adopted. The CFRP was cleaned using acetone.

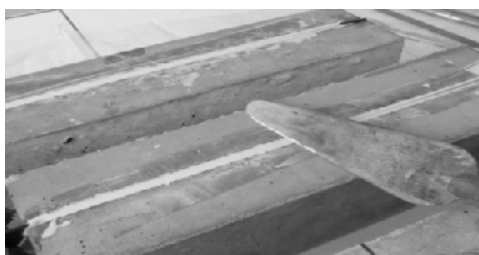


Fig.2 Strengthening of test specimens

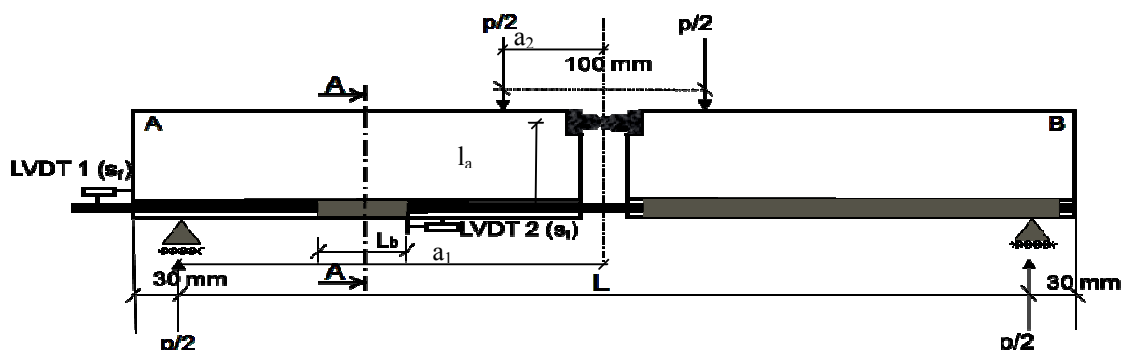


Fig.3 Pullout-bending test configuration

1. Configuration of the test system

The test layout adopted is similar to that proposed by RILEM [11] to evaluate the bond characteristics of conventional steel rebars. The pullout-bending test adopted in this work consists of two rectangular concrete blocks (A and B), connected through a steel hinge in the top part, and by the CFRP laminate or rod at the bottom, is stressed in simple bending (4 points) by two equal forces and arranged symmetrically about the midsection of the beam (Fig. 3). Subjecting the beam to a vertical load will cause traction in rod or plate. This allows an accurate calculation of tensile strength and stresses induced in the carbon rod and plate.

The bond test region was localized in block A, using distinct bond lengths,  $L_b$ . To ensure negligible slip of the plate or rod fixed to block B, a bond length of 320 mm was considered. This also ensures that the bond failure occurs in block A.

To measure the slip of the CFRP reinforcement, two displacement transducers (LVDT1 and LVDT2) of 10mm nominal stroke were applied (Figure 3). LVDT1 recorded the slip at the free end  $S_f$ , while LVDT2 measured the slip at the loaded end  $S_l$ .

2. General behaviour

Typical curves representing the pullout force versus slip at the loaded and free end are displayed in Figures 5 and 6 (for a bond length equal to 40 mm, and a C30 concrete strength).

The sequences observed are as follows: for loads less than 30% of the maximum pullout force ( $F_{max}$ ), no visible cracks occurred at the resin and concrete. Then, as the applied load increased, a first slip was recorded at the free end of the reinforcement.

Beyond  $0.4 F_{max}$ , the slip becomes increasingly nonlinear due to the plasticization of the epoxy resin, resulting in the separation process at the composite-resin and resin-reinforced concrete interfaces.

At the peak where the ultimate bond stress is reached, the slip increases brutally in both ends  $S_l$  and  $S_f$  of the reinforcement, and the curve drops in a nonlinear manner until the end point of rupture. This transition is due to the degradation of the mechanism of bond at the composite-resin-concrete interface.

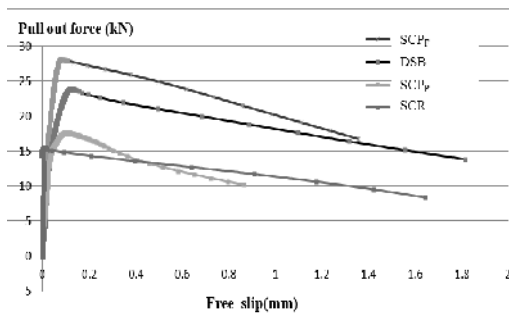


Fig.5. Typical Load-slip curves at free end

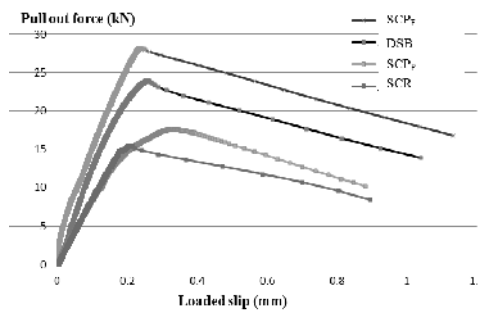


Fig.6. Typical Load-slip curves at loaded end

Different failure modes were observed such as: mixed interfacial failure (composite-epoxy/epoxy-concrete) with a concrete cracking forming a diagonal splitting cracks pattern as shown in Fig.7a, rupture of concrete surrounding the groove (Fig.7b), failure with facial slip between composite and epoxy (Fig.7c). Their occurrence depends on the considered parameters and in particular the bond length.

### B. Bond stress

The average ultimate bond stress was calculated by the following relations:

$$\tau_u = \frac{F_{max}}{\pi\phi L_b} \quad (SCR) \quad (2)$$

$$\tau_u = \frac{F_{max}}{2w_f L_b} \quad (SCP_F) \quad (3)$$

$$\tau_u = \frac{F_{max}}{w_f L_b} \quad (SCP_P) \quad (4)$$

Where:

- F<sub>max</sub>: the maximum applied pullout force (N);
- φ and w<sub>f</sub>: respectively the diameter of the rod (mm) and the width of the plate (mm);
- L<sub>b</sub>: the bond length (mm).

The results from the different test series are shown in Table III which also indicates the value of the pullout rigidity (K<sub>I</sub>), calculated by linear regression for loads between 20% and 80% of the tensile strength.

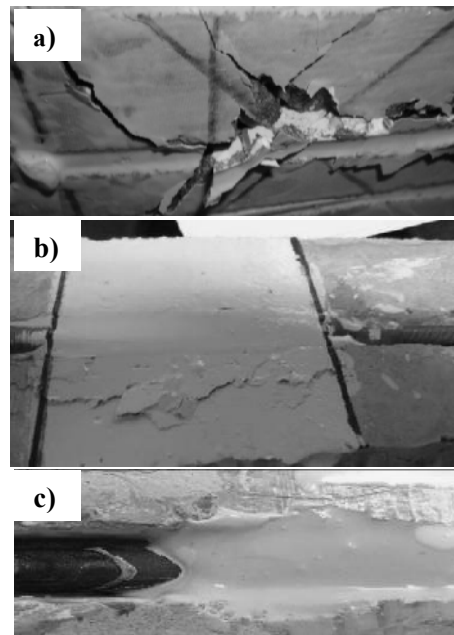


Fig.7. Bond failure modes

TABLE III  
RESULTS OF DIFFERENT SERIES

Designation	Concrete	L <sub>b</sub> (mm)	F <sub>max</sub> (kN)	τ <sub>u</sub> (MPa)	K <sub>I</sub> (kN/mm)
SCR	C30	40	16.55	16.47	26.20
SCR	C30	80	22.71	11.30	44.85
SCR	C30	120	33.37	11.07	68.05
SCR	C50	40	22.08	21.98	32.13
SCR	C50	80	30.57	15.21	55.11
SCR	C50	120	40.78	13.53	67.98
SCR	HPC75	40	23.01	22.90	48.28
SCR	HPC75	80	34.52	17.18	57.50
SCR	HPC75	120	46.02	15.27	74.88
DSB	C30	40	18.22	18.13	54.67
DSB	C30	80	26.60	13.24	59.39
DSB	C30	120	29.09	9.65	72.65
SCP <sub>F</sub>	C30	40	21.35	13.34	44.03
SCP <sub>F</sub>	C30	80	31.55	9.86	61.05
SCP <sub>F</sub>	C30	120	41.70	8.69	67.47
SCP <sub>F</sub>	C50	40	27.66	17.29	45.67
SCP <sub>F</sub>	C50	80	36.93	11.54	64.06
SCP <sub>F</sub>	C50	120	44.65	9.30	79.72
SCP <sub>F</sub>	HPC75	40	29.12	18.20	60.38
SCP <sub>F</sub>	HPC75	80	37.22	11.63	65.66
SCP <sub>F</sub>	HPC75	120	47.62	9.92	79.11
SCP <sub>P</sub>	C30	40	17.39	21.74	65.70
SCP <sub>P</sub>	C30	80	30.12	18.83	80.69
SCP <sub>P</sub>	C30	120	36.53	15.22	81.58

### 1) Effect of type of reinforcement

The maximum resistance obtained by the different configurations of composite strengthening is shown in Fig. 8. A better performance was achieved by of carbon plates (SCP<sub>F</sub> and SCP<sub>P</sub>) compared to carbon rods (SCR). For similar cross section, the reinforcement SCP<sub>F</sub> provides a greater contact surface area so that a greater pullout force is achieved. Although, the configuration SCP<sub>P</sub> has approximately the same contact surface as the configuration SCR, a greater resistance to pull out is recorded in this case.

This may be attributed to the smaller average thickness of the adhesive which best matches the reinforcement geometry and grooves.

The deformed steel bars present a rough surface allowing a better adhesion with surrounding concrete compared to SCP<sub>F</sub> and SCR. In this case, the ribs on the surface of the bars prevent the failure of a grip and the tensile strength of the reinforcement which limits pullout force. These results show a strong effect of the micro-geometry of the reinforcements.

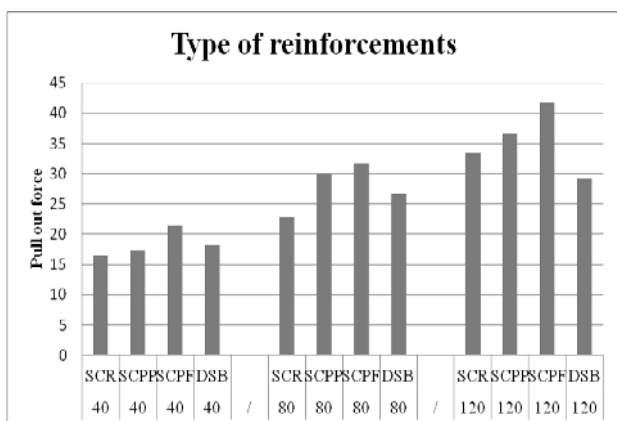


Fig.8. Effect of type of reinforcement for C30

2) Effect of bond length

The variation of the maximum pullout force regarding the increase of the bond length  $L_b$  is illustrated in Fig. 9. It is observed that the pullout force increases almost linearly with increasing bond length for the three types of concrete tested.

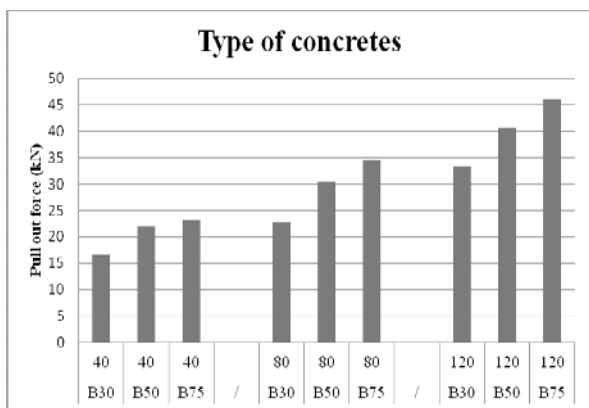


Fig.9 Effect of bond length for HPC75

3) Effect of concrete strength

In all cases, the resistance to pull out improves with increasing concrete strength as indicated by Fig. 10. This influence is more pronounced for smaller bond lengths ( $L_b=40$  mm). The optimum appears to be achieved with

$L_b=120$  mm, where the effect of concrete strength is reduced.

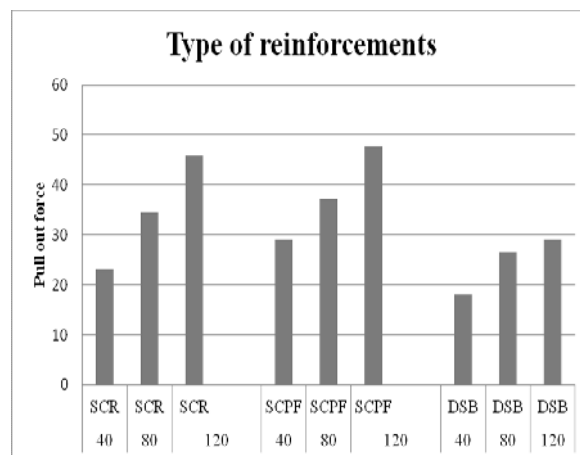


Fig.10 Effect of concrete strength for SCR

III. STUDY OF THE BENDING

The experimental study comprised a total of twelve (12) concrete beam-specimens initially reinforced with steel bars for flexural strength. In order to upgrade their flexural capacity, CFRP-NSM strengthening scheme was considered. All twelve beams were 1300 mm long and had a rectangular cross-section 180 mm high by 100 mm wide. Flexural reinforcement comprised 2 bars 8mm diameter for tension and for compression reinforcement, satisfying a minimum required steel ratio. To prevent shear failure from occurring prior to flexural failure, rectangular stirrups made of 6mm diameter were placed at every 30 mm in the shear zone. Fig. 11 depicts the geometric dimensions and reinforcing details of the typical beam specimen prior to upgrading.

Materials

A concrete with compressive strength of 39.76 MPa at 28 days has been used. The CFRP rod has a circular section of 8 mm diameter. The CFRP strip has a rectangular section 10 mm wide and 2.5 mm thick. For the epoxy to fill the groove, the product Sikadur-330 was used.

Table IV lists the experimental parameters. The unstrengthened control specimens have been cast to compare the strengthening performances of the various systems. The specimen designation is as follows: type of beam (C: control beam, U: upgraded beam), type of CFRP reinforcement (R: rod, S: strip), number of CFRP reinforcement (1 or 2) and state of shear stirrups (I: unchanged, II: partial cutting).

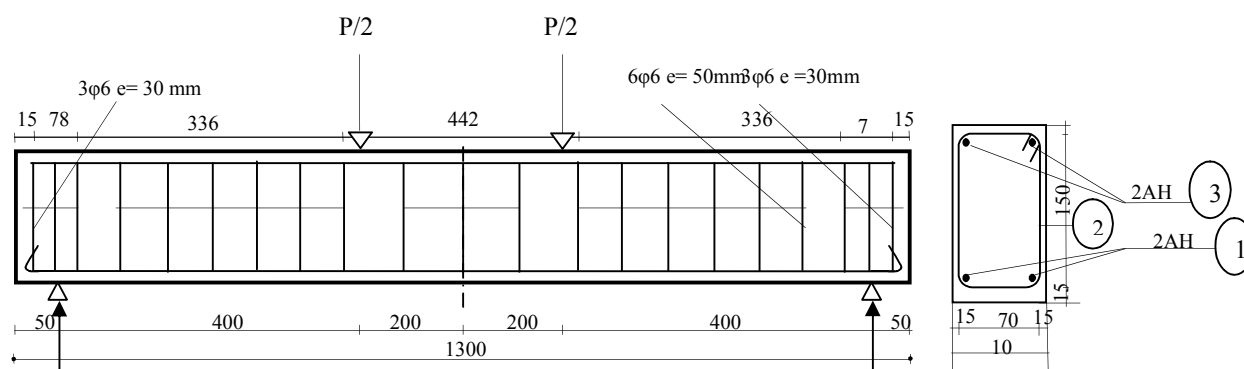


Fig. 11 Details and cross section of the specimen (mm)

Table IV lists the experimental parameters. The unstrengthened control specimens have been cast to compare the strengthening performances of the various systems. The specimen designation is as follows: type of beam (C: control beam, U: upgraded beam), type of CFRP reinforcement (R: rod, S: strip), number of CFRP reinforcement (1 or 2) and state of shear stirrups (I: unchanged, II: partial cutting).

Designation of specimens	CFRP Reinforcement
CB	Without
UBS1I	CFRP strip fully embedded
UBS2I	CFRP strip fully embedded
UBR1I	CFRP rods fully embedded
UBR2I	CFRP rods fully embedded
UBS1II	CFRP strip fully embedded with cutting off steel stirrups at bottom
UBS1I60	CFRP strip fully embedded

### 3. TEST RESULTS AND DISCUSSIONS

The test results in terms of applied load and deflection at cracking, at steel yielding, and at ultimate are summarized in Table V, along with a description of the failure mode.

TABLE V  
RESULTS OF DIFFERENT SERIES

Beam designation	Cracking load (kN)	Yielding load (kN)	Ultimate load (kN)	Strain at ultimate load (%)	Ultimate displacement (mm)	Failure mode
CB	07,94	17,99	23,24	7,55	18,21	Concrete compression
UBS1I	9,46	29,73	39,02	0,71	6,37	Concrete cover debonding
UBS2I	11,17	36,79	50,84	0,67	13,83	Concrete cover debonding
UBR1I	12,09	33,31	58,32	1,67	9,21	Concrete cover debonding
UBR2I	13,41	41,26	50,01	1,16	10,88	Concrete cover debonding
UBS1II	12,2	34,6	51,13	1,01	13,69	Concrete cover debonding

beams have failed in a compression concrete mode. The failure mode of all the strengthened beams was characterized by a CFRP debonding at the end of the beams accompanied with a concrete cover detachment all over its the middle. The sliding of the CFRP laminates started to be visible before the collapse of the strengthened beams. Test results highlighted the high potential of the innovative composite systems for

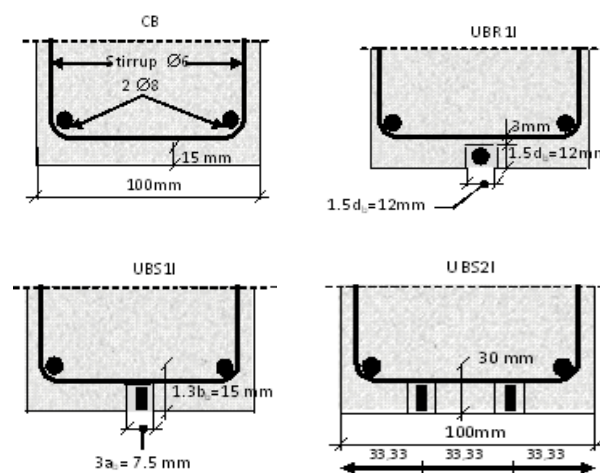


Fig. 12 Test variables

#### (i) Failure modes

The crack patterns on the reference beams basically consist of flexural cracks. The longitudinal steel bars in tension have yielded and the tests were interrupted when the deflection at mid span was greater than 20mm. Therefore, the reference

flexural strengthening applications and similar effectiveness compared with externally bonding the reinforcement.

In all the cases considered failure occurred after yielding of the existing tension steel. The reinforcement with NSM bars has enhanced the performances of the strengthened beams both in terms of failure load and deflection.

## (ii) Load–deflection relationship

The force-deflection relationships for the series of tested beams are depicted in Figure 13, and the main results are presented in Table V. It is observed that a double amount of the ultimate load of the corresponding reference beam was practically achieved. The increase on the load at the onset of yielding the steel reinforcement (yielding load) was also significant, varying from 32% to 47%. The displacement corresponding yielding and ultimate loads showed a minimum decrease of 45% and 47%, respectively regarding control beams. All the tested strengthened beams showed higher stiffness than their corresponding reference beams. The ultimate load for the strengthened beams was also increased attaining a maximum increase of 250%.

The control beams illustrate a typical behavior of a ductile section. For smaller load, they showed linear elastic deformation with a tendency to accelerate after the cracking load. After yielding, the beams displayed a significant amount of ductility. In general, almost all strengthened beams showed a linear curve regarding their load-deflection behavior with a smaller ductility.

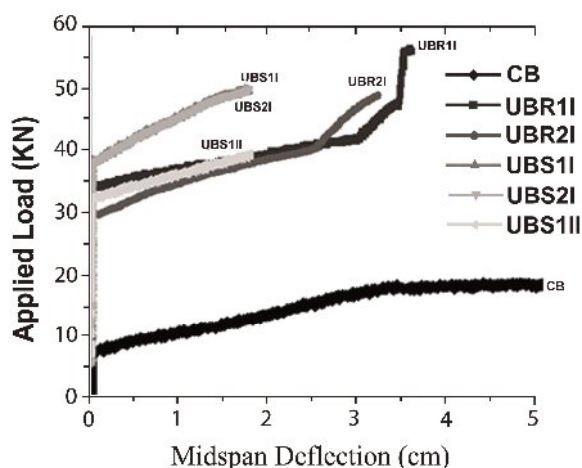


Fig.13 Load deflection relationship

## IV. CONCLUSION

Bond tests were performed by bending to characterize the bond behavior of carbon reinforcements positioned in the concrete by the NSM method. An experimental program has been also carried out to evaluate the response of RC beams strengthened in flexure with NSM FRP reinforcement. Various parameters were considered. From the results obtained, the following comments can be made:

A better performance was achieved by of carbon plates compared to carbon rods.

The pullout force increases almost linearly with the bond length for the three types of concrete tested.

The resistance to pull out improves with increasing concrete strength and this influence is more pronounced for smaller bond lengths.

The strengthening of RC beams using NSM CFRP rods improved the ultimate load and deflection. The flexural

stiffness of strengthened beams increased in the elastic field and a high ultimate load capacity was recorded.

The failure mechanisms were governed for all beams by the collapse of compressive concrete and CFRP debonding at the end of the beams accompanied with a concrete cover detachment all over its the middle.

We also notice that the use of the CFRP rod is better than of the strip CFRP.

The experimental results show clearly the effectiveness of the proposed strengthening solution. The mechanical performances (ultimate load, overall stiffness, steel yielding) comparatively to the reference beam (concrete reinforced beam) were improved significantly.

## REFERENCES

- [1] J.A.O., Barros, A.S. Fortes, "Concrete beams reinforced with carbon laminates bonded into slits", in *Proceedings of 5º Congreso de Métodos Numéricos en Ingeniería*, Madrid, Spain, 2002, pp.1-6.
- [2] De. Lorenzis, J.G. Teng, "Near-surface mounted FRP reinforcement: An emerging technique for strengthening structures", Department of Innovation Engineering, University of Lecce, via per Monteroni, 73100 Lecce, Italy, Oct. 2006.
- [3] J.A.O. Barros \*, A.S. Fortes ,Flexural strengthening of concrete beams with CFRP laminates bonded into slits *Cement & Concrete Composites*, 27 (2005) 471–480
- [4] A Kamiharako, T. Shimomura, K. Maruyama, H. Nishida, "Stress transfer and peeling-off behaviour of continuous fiber reinforced sheet-concrete system". In *Proc. 7<sup>th</sup> East Asia-Pacific Conference on Structural Engineering and Construction*; Tokyo, 1999. pp. 1283–1288.
- [5] J.M., Sena Cruz, J.A.O., Barros, R. Gettu, "Bond behavior of near-surface mounted CFRP laminate strips under monotonic and cyclic loading." Rep. DEC/E-04, Department of Civil Engineering, University of Minho, Guimarães, Portugal, 55 pp. 2004.
- [6] F. Al-Mahmoud, A. Castel, R.I François, C. Tourneur, "RC beams strengthened with NSM CFRP rods and modeling of peeling-off failure", *Composite Structures*, Vol. 92, pp. 1923-1930, Jul. 2010.
- [7] F. Sayed Ahmad, G. Foret, R. Le Roy, "Bond between carbon fibre-reinforced polymer (CFRP) bars and ultra high performance fibre reinforced concrete (UHPC): Experimental study", *Construction and Building Materials*, vol. 25, pp. 479-485, Feb. 2011.
- [8] Kotynia R. Strengthening of reinforced concrete structures with near surface mounted FRP reinforcement. In: Proc. 5th int. conf. AMCM (CD-ROM), Gliwice – Ustrum, Poland; 2005.
- [9] El-Hacha R, Rizkalla S. Near-surface mounted fiber reinforced polymer reinforcements for flexural strengthening of concrete structures. *ACI Struct J* 2004;101(5):717–26.
- [10] Kishi N, Mikami H, Kurihashi Y, Sawada S. Flexural behaviour of RC beams reinforced with NSM AFRP rods. In: Proc. int. symposium BBFS; 2005. p. 337.
- [11] RILEM. "Bond test for reinforcement steel. Beam test." TC9-RC, 1982.